Intracavity-Pumped, Cascaded Mid-IR Optical Parametric Oscillator Based on AgGaSe2

CONFERENCE PAPER · OCTOBER 2015

DOI: 10.1364/ASSL.2015.ATh2A.19

7 AUTHORS, INCLUDING:

Georgi Marchev

49 PUBLICATIONS **288** CITATIONS

SEE PROFILE

Dmitry Kolker

Novosibirsk State Technical University

36 PUBLICATIONS **145** CITATIONS

SEE PROFILE

Andrius Zukauskas

KTH Royal Institute of Technology

38 PUBLICATIONS **90** CITATIONS

SEE PROFILE

Nadezhda Kostyukova

Novosibirsk State Technical University

14 PUBLICATIONS **4** CITATIONS

SEE PROFILE

Intracavity-Pumped, Cascaded Mid-IR Optical Parametric Oscillator Based on $AgGaSe_2$

Andrey A. Boyko,[1,2,3] Georgi M. Marchev,[1] Valentin Petrov,[1] Valdas Pasiskevicius,[4] Dmitry B. Kolker,[3] Andrius Zukauskas,[4] Nadezhda Y. Kostyukova[2,3]

[1]*Max-Born-Institute for Nonlinear Optics and Ultrafast Spectroscopy, 2A Max-Born-Str., D-12489 Berlin, Germany,*
[2]*Special Technologies, Ltd., 1/3 Zeljonaja gorka Str., 630060 Novosibirsk, Russia,*
[3]*Research Laboratory of Quantum Optics Technology, Novosibirsk State University, 2 Pirogova Str., 630090 Novosibirsk, Russia,*
[4]*Department of Applied Physics, Royal Institute of Technology, 10691 Stockholm, Sweden,*
baa.nsk@gmail.com

Abstract: We report on an $AgGaSe_2$ optical parametric oscillator (OPO), intracavity pumped by the 1.85-μm signal pulses from a 1.064-μm pumped Rb:PPKTP OPO. It operates at 100 Hz with idler tunability from 5.8 to 8.3 μm.

OCIS codes: (190.4970) Parametric oscillators and amplifiers; (160.4330) Nonlinear optical materials.

1. Introduction

Cascaded or tandem optical parametric oscillators (OPOs) for down conversion of laser radiation into the mid-IR spectral range using non-oxide nonlinear crystals in the second stage have rarely been realized with intracavity pumping [1]. Apart from more compact and robust design such schemes profit from the higher intracavity pump power (signal or idler wave of an oxide based OPO pumped usually at 1.064 μm by a Nd:YAG laser system). Compared to pumping inside the cavity of a ns laser (demonstrated in the past with CdSe or $ZnGeP_2$ (ZGP) in a gain-switched Cr:ZnSe laser [2,3] or more recently with orientation-patterned GaAs (OPGaAs) in a Q-switched Tm:YAP laser [4]), the cascaded OPO approach offers the flexibility of selecting the most suitable pump wavelength for broadband tunability of the second stage based on a specific non-oxide nonlinear crystal [1]. The first such realization at a repetition rate of 5 Hz, with a doubly-resonant OPO (DRO) based on ZGP pumped by the o-beam of a near-degenerate, double pump-pass, type-II KTP DRO resulted in an overall conversion efficiency of 5.2% from 1.064 μm to the mid-IR (combined signal and idler energy near degeneracy at 4.2 μm) [5]. A similar scheme with a near-degenerate ZGP DRO operating at 5 kHz was presented in [6]. In the present work we investigate a singly-resonant OPO (SRO) based on an $AgGaSe_2$ (AGSe) crystal intracavity pumped at 1.85 μm by the signal pulses of a Rb:PPKTP DRO. Both the choice of a SRO design and the transparency of the AGSe crystal enable coverage of much broader portions of the mid-IR spectral range, in principle at least up to ~14 μm.

2. Experimental set-up and Rb:PPKTP DRO performance

The Rb:PPKTP crystal employed in the first stage was 12-mm long (x-direction, propagation), 8-mm wide (y-direction) and 5-mm thick (z-direction, poling). The metal electrode grating used had a period of Λ=38.5 μm and was 8 mm long by 5 mm wide. Thus the useful aperture of this uncoated sample was ~5×5 mm^2. The pump source was a diode-pumped multi longitudinal mode, Q-switched at 100 Hz, Nd:YAG laser / amplifier, Fig. 1(a). To improve the spatial beam profile (eliminate diffraction rings producing hot spots) a vacuum diamond pinhole was installed in the focus of an expanding telescope. The pump M^2 parameter measured behind the telescope amounted to ~2. The beam size was then reduced by an additional telescope, Fig. 1(a), to a Gaussian diameter (at e^{-2} intensity level) of 2.9 mm in the horizontal and 3.6 mm in the vertical (along the polarization) directions. The dichroic mirror DM1 totally reflects the pump (P_1) radiation and highly transmits both signal (S_1) and idler (I_1) from the first stage. The ZnSe input-output coupler (IOC) of the first OPO is highly transmitting for P_1, highly reflecting for S_1 but not optimized (transmitting 55%) for I_1. Thus using a cut-on filter, only the idler, I_1 in Fig. 1(a), from the first stage is monitored at this output. DM2 is highly reflecting both for the fundamental (1.064 μm) and the second-harmonic of the pump laser and highly transmitting the s-polarized S_1 (96%) and I_1 (91%) waves. DM3 is at 50 mm (physical length) from the IOC and highly reflects P_1 but transmits the second harmonic. Thus a double pump pass in the Rb:PPKTP crystal is realized while the green light parasitically generated in it does not reach the AGSe crystal. The Rb:PPKTP DRO physical cavity length amounts to 103 mm (arm containing the AGSe crystal) and 88 mm (main idler I_1 beam arm). The physical cavity length of the AGSe SRO is 62 mm. The performance of the Rb:PPKTP DRO improved both in terms of output power and beam divergence when an RC = -1 m Au mirror was used as a total reflector (instead of a plane mirror). The signal of the AGSe SRO (S_2) is resonated between this mirror and the highly reflecting ZnSe output coupler (OC) which transmits 76±5% in the idler (I_2) spectral tuning range.

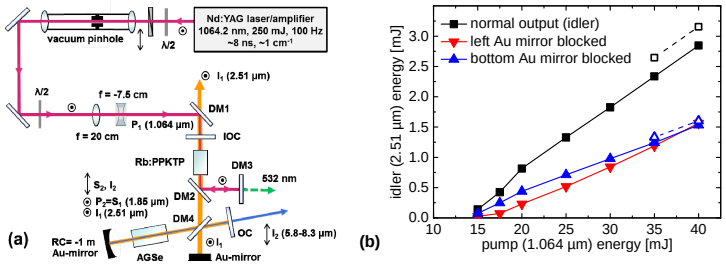

Fig. 1. Schematic of the intracavity pumped, cascaded AGSe OPO (a), and performance of the first stage (idler I_1) without the AGSe crystal using two plane Au-mirrors (solid lines and full symbols) and substituting the left one (the one in the AGSe arm) by an RC = -1 m Au-mirror (dashed lines and open symbols) (b). The data in (b) are corrected for the 91% transmission of DM1.

The dichroic CaF_2 mirror DM4 totally reflects S_1=P_2 but is not optimized near 2.5 μm (I_1 and S_2), where the transmission achieved at 50° angle of incidence is ~70% (both s- and p-polarizations), and for I_2, for which the transmission is 80±5%. Thus I_1 is partially resonated also in the arm containing the AGSe crystal while S_2 and I_2 experience some reflection losses. The performance of the Rb:PPKTP DRO with this cavity but with the AGSe crystal removed is shown in Fig. 1(b). At room temperature the signal S_1 was at 1.85 μm and the idler I_1 - at 2.51 μm. The measurable output behind IOC and DM1 consists mainly of the idler and is obviously not optimized for this configuration designed for intracavity pumping. Nevertheless, it is seen from the figure that both arms containing the Au-mirrors provide feedback for the idler I_1. Figure 1(b) shows also the improvement achieved when the plane Au-mirror in the signal S_1 arm was substituted by a curved mirror. This also reduced the divergence of the S_1 beam matching it to the angular acceptance of the AGSe crystal which is ~4 mrad. Using the 4% leakage of S_1 though the IOC, at 40 cm from it we measured a spot size diameter of 4 and 5 mm in the horizontal and vertical direction, respectively. The maximum I_1 output energy measured (3.16 mJ) leads to an estimate of 7.8 mJ for the intracavity S_1 energy that will be used for pumping the second AGSe stage, and P_1 (1.064 μm) depletion of 34%. With an extrapolated threshold of 10 mJ (Fig. 1(b)) the total (S_1 and I_1) internal slope efficiency amounts to 45%.

3. Performance of the AGSe SRO at 100 Hz

The type-I AGSe sample (φ=45°, θ=52°) available for the present experiment was 14-mm long with an aperture of 4.5×4.5 mm^2. It was AR-coated for S_1=P_2 (94% transmission) but had also high transmission (87%) for S_2/I_1 while in the I_2 spectral range the measured transmission was 70%. The idler I_2 was extracted after a double pass through the crystal.

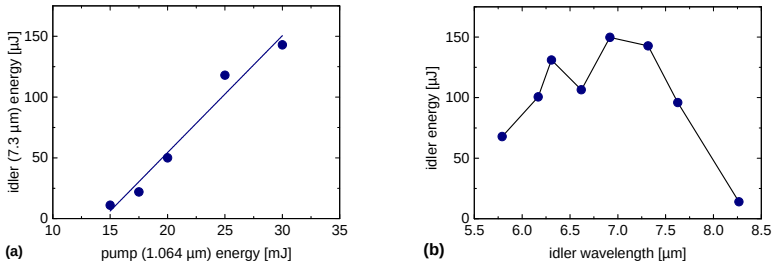

Fig. 2. Idler I_2 energy of the AGSe SRO at 7.3 μm in dependence on the pump P_1 energy at 1.064 μm (a), and angle tuning of the AGSe SRO in the mid-IR at a pump energy of 30 mJ at 1.064 μm.

Figure 2(a) shows the input-output characteristics of the cascaded OPO for an idler I_2 wavelength of 7.3 μm. The maximum output energy of 143 μJ obtained is roughly 15 times higher than the energy specified in [5] at the upper wavelength limit of ZGP. In terms of average power (14.3 mW) the improvement we have achieved is ~300 times. Note that, operation at such long wavelengths was not reported in [6]. The angle tuning results for the AGSe SRO are summarized in Fig. 2(b). They are determined to a great extent by the crystal cut selected. However, an important portion of the spectrum interesting for minimally invasive surgery is covered for the present selection [7].

Figure 3 shows the spectro-temporal characteristics measured. The pulse shapes depicted in Fig. 3(a) are arbitrarily normalized to a common maximum. The depletion of the P_2 pulse can be seen when the AGSe SRO is operating. In general all pulses are shorter than the 8-ns P_1 (1.064 μm) pump. However, while the traces in the near-IR were measured with a 70 ps response InGaAs photodiode, the mid-IR idler I_2 was measured by a (HgCdZn)Te

detector with a rise time of 2 ns and the measurement was not corrected for this finite response. Nevertheless this pulse (FWHM of 6.5 ns) is also shorter than the 1.064 µm pump pulse.

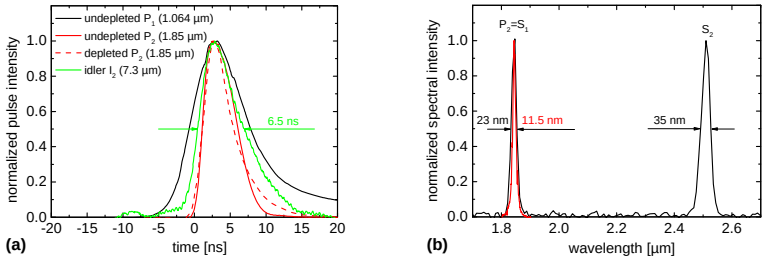

Fig. 2. Temporal shapes of the pump laser pulse at 1.064 µm (P_1), the P_2=S_1 pulse without the AGSe crystal and with the second stage operating, and the idler I_2 pulse at 7.3 µm (a). Low resolution spectra of the P_2=S_1 and S_2 pulses (black lines) at maximum power and high resolution spectrum of the P_2=S_1 pulses (red line) (b).

Figure 3(b) shows the spectra of the pump (P_2=S_1) and signal (S_2) pulses of the AGSe SRO. With a low resolution PbS spectrometer the P_2=S_1 spectrum at 1.85 µm is not well resolved but the FWHM of 23 nm gives an idea about the resolution for the S_2 spectrum at ~2.5 µm measured simultaneously. Independent measurement of the P_1 (1.064 µm) spectrum yields a spectral resolution of ~15 nm for this spectrometer. The correct bandwidth of the P_2=S_1 spectrum was measured by an InGaAs spectrometer yielding a FWHM of 11.5 nm, see Fig. 3(b). This is roughly 2 times narrower than the 25 nm OPO bandwidth acceptance calculated for PPKTP assuming monochromatic pump. This can be explained by spectral narrowing in the Rb:PPKTP OPO. On the other hand, the measured P_2 spectral bandwidth is roughly 3 times larger than the calculated pump spectral acceptance of the AGSe crystal (4 nm). However, such a calculation assumes monochromatic S_2 radiation which is not true for the AGSe SRO where the signal wavelength is not fixed by a spectrally selective element. Thus, this effect is not considered to be a serious limiting factor. Though strictly speaking the FWHM of the S_2 pulses of 35 nm in Fig. 3(b) is an upper limit, with a spectral resolution of 15 nm it is very close to the actual bandwidth. By convolution of the two spectra (pump and signal) one obtains a spectral bandwidth (FWHM) of 65 cm^{-1} for the idler I_2 or about 340 nm at 7.3 µm.

4. Conclusion

In conclusion, we investigated an intracavity-pumped, cascaded AGSe OPO generating idler pulses in the 5.8-8.3 µm spectral range. The maximum mid-IR pulse energy at 100 Hz reached 150 µJ near 7 µm. Maximized extraction of this idler I_2 (through optimized mirrors DM4 and OC) alone would increase this level to about 250 µJ. Further increase of the overall efficiency can be expected by improved characteristics of DM4 at I_1 and S_2 (maximum transmission) as well as of IOC at I_1 (maximum reflection). In this case only the depletion in the AGSe crystal will play the role of a loss mechanism for the Rb:PPKTP DRO. Power scaling can be achieved increasing the beam sizes while extending the tuning range towards longer wavelengths in the mid-IR is possible with different AGSe crystals and a ZnSe substrate for DM4. Such experiments are planned and will be reported at the conference.

References:

1. V. Petrov, "Frequency down-conversion of solid-state laser sources to the mid-infrared spectral range using non-oxide nonlinear crystals, " *Progress Quantum Electron.* **42**, 1-106 (2015).
2. A. Zakel, G. J. Wagner, W. J. Alford, and T. J. Carrig, "High-power, rapidly-tunable dual-band CdSe optical parametric oscillator," Conference on Lasers and Electro-Optics, CLEO 2005, OSA Technical Digest CD ROM, paper CThY5.
3. A. Zakel, G. J. Wagner, W. J. Alford, and T. J. Carrig, "High-power, rapidly-tunable $ZnGeP_2$ intracavity optical parametric oscillator," Advanced Solid-State Photonics, ASSP 2005, OSA TOPS Vol. 98, paper MD5, pp. 433-437.
4. D. J. Kane, J. M. Hopkins, M. H. Dunn, P. Schunemann, and D. J. M. Stothard, "Tm:YAP pumped intracavity pulsed OPO based on orientation-patterned gallium arsenide (OP-GaAs)," 6th EPS-QEOD Europhoton Conference on Solid-State, Fibre and Waveguide Coherent Light Sources, 2014, paper TuA-T1-O-03.
5. P. B. Phua, K. S. Lai, R. F. Wu, and T. C. Chong, "Coupled tandem optical parametric oscillator (OPO): an OPO within an OPO," *Opt. Lett.* **23**, 1262-1264 (1998).
6. R. Wu, K. S. Lai, W.-P. E. Lau, H. F. Wong, Y. L. Lim, K. W. Lim, and L. C. L. Li, "A novel laser integrated with a coupled tandem OPO configuration," Conference on Lasers and Electro-Optics, CLEO 2002, OSA Technical Digest, p. 154, paper CTuD6.
7. G. S. Edwards, R. H. Austin, F. E. Carroll, M. L. Copeland, M. E. Couprie, W. E. Gabella, R. F. Haglund, B. A. Hooper, M. S. Hutson, E. D. Jansen, K. M. Joos, D. P. Kiehart, I. Lindau, J. Miao, H. S. Pratisto, J. H. Shen, Y. Tokutake, A. F. G. van der Meer, and A. Xie, "Free-electron-laser-based biophysical and biomedical instrumentation," *Rev. Sci. Instrum.* **74**, 3207-3245 (2003).